Minerals **2013**, *3*, 94-120; doi:10.3390/min3010094

OPEN ACCESS

minerals

ISSN 2075-163X
www.mdpi.com/journal/minerals

Article

Three Compositional Varieties of Rare-Earth Element Ore: Eudialyte-Group Minerals from the Norra Kärr Alkaline Complex, Southern Sweden

Axel S.L. Sjöqvist [1,*], David H. Cornell [1], Tom Andersen [2], Muriel Erambert [2], Mattias Ek [1] and Magnus Leijd [3]

[1] Department of Earth Sciences, University of Gothenburg, PO Box 460, SE-405 30 Göteborg, Sweden; E-Mails: cornell@gvc.gu.se (D.H.C.); mattias.ek@erdw.ethz.ch (M.E.)
[2] Department of Geosciences, University of Oslo, PO Box 1047 Blindern, N-0316 Oslo, Norway; E-Mails: tom.andersen@geo.uio.no (T.A.); m.m.l.erambert@geo.uio.no (M.E.)
[3] Tasman Metals Ltd., Skiftesvägen 14, SE-563 31 Gränna, Sweden; E-Mail: magnus.leijd@tasmanmetals.se

* Author to whom correspondence should be addressed; E-Mail: axel@student.gu.se; Tel.: +46-703-599-245.

Received: 8 December 2012; in revised form: 18 January 2013 / Accepted: 25 February 2013 / Published: 20 March 2013

Abstract: Agpaitic nepheline syenites at the Norra Kärr Alkaline Complex, southern Sweden, are rich in zirconium and rare-earth elements (REE), which are mainly accommodated in eudialyte-group minerals (EGM). Norra Kärr hosts three compositionally distinct groups of EGM, which are complex zirconosilicates. Analyses of EGM by electron beam energy-dispersive (SEM-EDS) and wavelength-dispersive (WDS-EMP) X-ray microanalysis are presented and compared, complemented by whole-rock analyses. The SEM-EDS and WDS-EMP methods produce comparable results for most elements. Considering that most SEM instruments have a user-friendly EDS system, it is a useful tool for reconnaissance work in research and especially in exploration-related studies. The EGM evolved markedly from an initial Fe-rich and REE-poor, but HREE-dominated variety, to an intermediate Fe-Mn and HREE-rich one, and to a final Mn- and LREE-rich variety, which occur in rocks classified as lakarpite and grennaite. Based on the Mn/(Fe+Mn) ratios of the EGM, this trend is interpreted as a result of magmatic evolution. The threefold diversity of EGM presented in this work is much broader than has previously been documented.

Keywords: eudialyte-group minerals; agpaitic rocks; nepheline syenite; rare-earth elements; Norra Kärr Alkaline Complex; SEM-EDS; WDS-EMP

1. Introduction

1.1. Agpaitic Rocks and Their Mineralogy

Agpaitic rocks are peralkaline nepheline syenites, characterised by the presence of complex zirconosilicate minerals such as eudialyte, catapleiite, and members of the wöhlerite and rosenbuschite groups as rock-forming minerals (see Table 1 for the chemical formulae of relevant minerals). Agpaitic rocks generally contain high concentrations of otherwise rare elements such as Li, Be, High Field Strength Elements (HFSE; e.g., Zr, Nb, Ta, REE, Y), and volatiles F and Cl [1].

Table 1. A list of relevant minerals mentioned in this article.

Mineral	Formula
Arfvedsonite	$[Na][Na_2][Fe^{2+}_4 Fe^{3+}]Si_8O_{22}(OH)_2$
Catapleiite	$Na_2ZrSi_3O_9 \cdot H_2O$
Eckermannite [1]	$[Na][Na_2][(Mg,Fe^{2+})_4Al](Si_8O_{22})(OH)_2$
Lorenzenite	$Na_2Ti_2(Si_2O_6)O_3$
Mosandrite [2]	$Ti(\square,Ca,Na)_3(Ca,REE)_4(Si_2O_7)_2(H_2O,OH,F)_4 \cdot \sim 1H_2O$
Pectolite	$NaCa_2(HSi_3O_9)$
Rosenbuschite	$(Ca,Na)_3(Zr,Ti)Si_2O_7FO$
Willemite	Zn_2SiO_4
Wöhlerite	$NaCa_2(Zr,Nb)(Si_2O_7)(O,OH,F)_2$

Notes: Chemical formulae were retrieved from the Mindat.org mineral database [2] unless otherwise noted; □: vacancy; [1] The Norra Kärr Alkaline Complex is the type locality for this mineral; [2] Bellezza *et al.* [3].

The original definition of agpaitic rocks by Ussing [4] required whole-rock molar proportions of (Na + K)/Al ≥ 1.2. This ratio is known as the agpaitic index (A.I.) or peralkaline index (P.I.). Sørensen [5] introduced an alternative definition, based on the presence of complex Na-Ca-Ti-Zr-silicates instead of, e.g., zircon and ilmenite; which is accepted in current petrographic nomenclature [6]. For a full review of the nomenclature of agpaitic nepheline syenites, see Sørensen [7]. Recently, Marks *et al.* [8] suggested that rocks other than nepheline syenites, with similar Ti-Zr mineralogy, should be included as agpaitic rocks (e.g., eudialyte- and elpidite-bearing granites).

The type locality for agpaitic rocks is the Ilímaussaq alkaline complex in southern Greenland [4,9,10] (and references therein), which contains different agpaitic nepheline syenites such as foyaite, naujaite, kakortokite, and lujavrite. Other important localities of agpaites are the Khibina and Lovozero complexes, Kola Peninsula, Russia [11], the Mont Saint-Hilaire complex, Quebec, Canada [12,13], parts of the Tamazeght complex, Morocco [14], the Pilanesberg complex, South Africa [15], and the pegmatites at Langesundsfjord, Norway [16,17].

Agpaitic magmas may originate by extreme crystal fractionation of mantle-derived alkali basaltic magma (producing a characteristic negative europium anomaly) or nephelinitic magma (without europium anomaly) deep in the crust [1], which gives rise to their exotic chemistry and mineralogy.

1.2. Eudialyte-Group Minerals

Eudialyte has its type locality at Kangerdluarssuk, in the Ilímaussaq alkaline complex, south Greenland ([18], Stromeyer, 1819 in [19]). The eudialyte group presently counts 26 Na-zirconosilicate minerals [20] that incorporate variable amounts of Ca, Fe, Mn, REE, Sr, Nb, Ta, K, Y, Ti, W, and H [19]. See Table 2 for chemical formulae and site occupancies in Table 3 for relevant EGM. The IMA-accepted general formula for the eudialyte group [19,21] is:

$N_{15}[M(1)]_6[M(2)]_3[M(3)][M(4)]Z_3(Si_{24}O_{72})O'_4X_2$, with
N = Na, Ca, K, Sr, REE, Ba, Mn, H_3O^+;
$M(1)$ = Ca, Mn, REE, Na, Sr, Fe;
$M(2)$ = Fe, Mn, Na, Zr, Ta, Ti, K, Ba, H_3O^+;
$M(3, 4)$ = Si, Nb, Ti, W, Na;
Z = Zr, Ti, Nb;
O' = O, OH^-, H_2O;
X = H_2O, Cl^-, F^-, OH^-, CO_3^{2-}, SO_4^{2-}, SiO_4^{4-}.

Table 2. Eudialyte-group minerals mentioned in this article.

Mineral	Formula
Eudialyte	$Na_{15}Ca_6(Fe,Mn)_3Zr_3Si(Si_{25}O_{73})(O,OH,H_2O)_3(OH,Cl)_2$
Ferrokentbrooksite	$Na_{15}Ca_6Fe_3Zr_3Nb(Si_{25}O_{73})(O,OH,H_2O)_3(F,Cl)_2$
Kentbrooksite	$Na_{15}Ca_6Mn_3Zr_3Nb(Si_{25}O_{73})(O,OH,H_2O)_3(F,Cl)_2$
Oneillite	$Na_{15}Ca_3Mn_3Fe_3Zr_3Nb(Si_{25}O_{73})(O,OH,H_2O)_3(OH,Cl)_2$
Zirsilite-(Ce)	$(Na,\square)_{12}(REE,Na)_3Ca_6Mn_3Zr_3Nb(Si_{25}O_{73})(OH)_3(CO_3)\cdot H_2O$

Note: Formulae from Johnsen *et al.* [19].

Table 3. Predominant occupancy in the non-silicate sites of the eudialyte-group minerals [19].

Mineral	*M*(1,1b)	*M*(1a)	*M*(2)	*M*(3)	*M*(4)	*N*(1,2,3,5)	*N*(4)	*X*
Eudialyte	Ca		Fe	Si	Si	Na	Na	Cl
Ferrokentbrooksite	Ca		Fe^{2+}	Nb	Si	Na	Na	Cl
Kentbrooksite	Ca		Mn	Nb	Si	Na	Na	F
Oneillite	Ca	Mn	Fe	Nb	Si	Na	Na	OH
Zirsilite-(Ce)	Ca		Mn	Nb	Si	Na	REE	CO_2, OH

The crystal structure of eudialyte-group minerals is based on a trigonal network comprising a nine-membered silica ring (Si_9O_{27}) combined with a six-membered ring of calcium octahedra (Ca_6O_{24}). These are held together by zirconium octahedra (ZrO_6) with three-membered silica rings (Si_3O_9). Various sites in the crystal structure can accommodate a third of the periodic table [22]. The complex crystallography has made it difficult to find stoichiometric crystal-chemical constants, however

Johnsen and Grice [23] proposed to normalize EGM formulae to Si + Al + Zr + Ti + Hf + Nb + W + Ta = 29 *apfu* (atoms per formula unit) based on the crystallography and electron-microprobe analyses.

The Mn/Fe ratio of eudialytes has been suggested as a monitor for magmatic evolution by various authors [21,24–26]. Generally, early- to late-magmatic eudialytes show increasing Mn/Fe ratios [21], controlled by factors such as the co-fractionation of Fe-rich clinopyroxene and amphibole.

In this work we present new chemical analyses of whole rocks and eudialyte from the Norra Kärr Alkaline Complex, southern Sweden. Two electron-beam microanalytical methods are evaluated and compared. Norra Kärr has been known for eudialyte- and catapleiite-bearing varieties of nepheline syenite since the early 1900s [27] and is recognized as one of the classic agpaitic complexes, but due to limited research efforts it remains relatively poorly understood.

One well-known outcrop at Norra Kärr is particularly rich in pink eudialyte and professionals and amateurs alike have traditionally collected specimens of "Norra Kärr eudialyte" at this outcrop: the "Discovery outcrop" (Figure 1). A web search [28] on "eudialyte Norra Kärr" produces many images of vibrantly pink eudialyte, mostly from this outcrop. The scientific literature contains several Norra Kärr eudialyte analyses [21,27,29], presented as representative but without naming the locality.

Recent drilling by Tasman Metals Ltd. has provided the extensive sample set used in this work. We have been able to characterize the overall variation in eudialyte composition and to provide more representative data for eudialyte from the Norra Kärr Alkaline Complex.

Figure 1. The "Discovery outcrop" (58°6.2' N, 14°34.1' E), where most workers collected their samples of "Norra Kärr eudialyte". The rock hammer's handle is about 0.75 m long.

1.3. The Norra Kärr Alkaline Complex

The Norra Kärr Alkaline Complex (in short "Norra Kärr") is a small Proterozoic peralkaline intrusion, which was discovered at Norra Kärr farm during regional bedrock mapping by the Swedish Geological Survey (SGU) and first described in 1906 by Törnebohm [27]. The intrusion is roughly elliptical (1200 m × 400 m) with the long axis aligned approximately north-south and is located about 1 km east of lake Vättern (58°06' N, 14°40' E; Figure 2). The general dip is approximately 45° to the west.

Figure 2. Simplified geologic map of the Norra Kärr Alkaline Complex, produced by Tasman Metals Ltd., and Norra Kärr's location on a generalized geologic map of southern Scandinavia. Sample locations in specific drill holes are marked on the map.

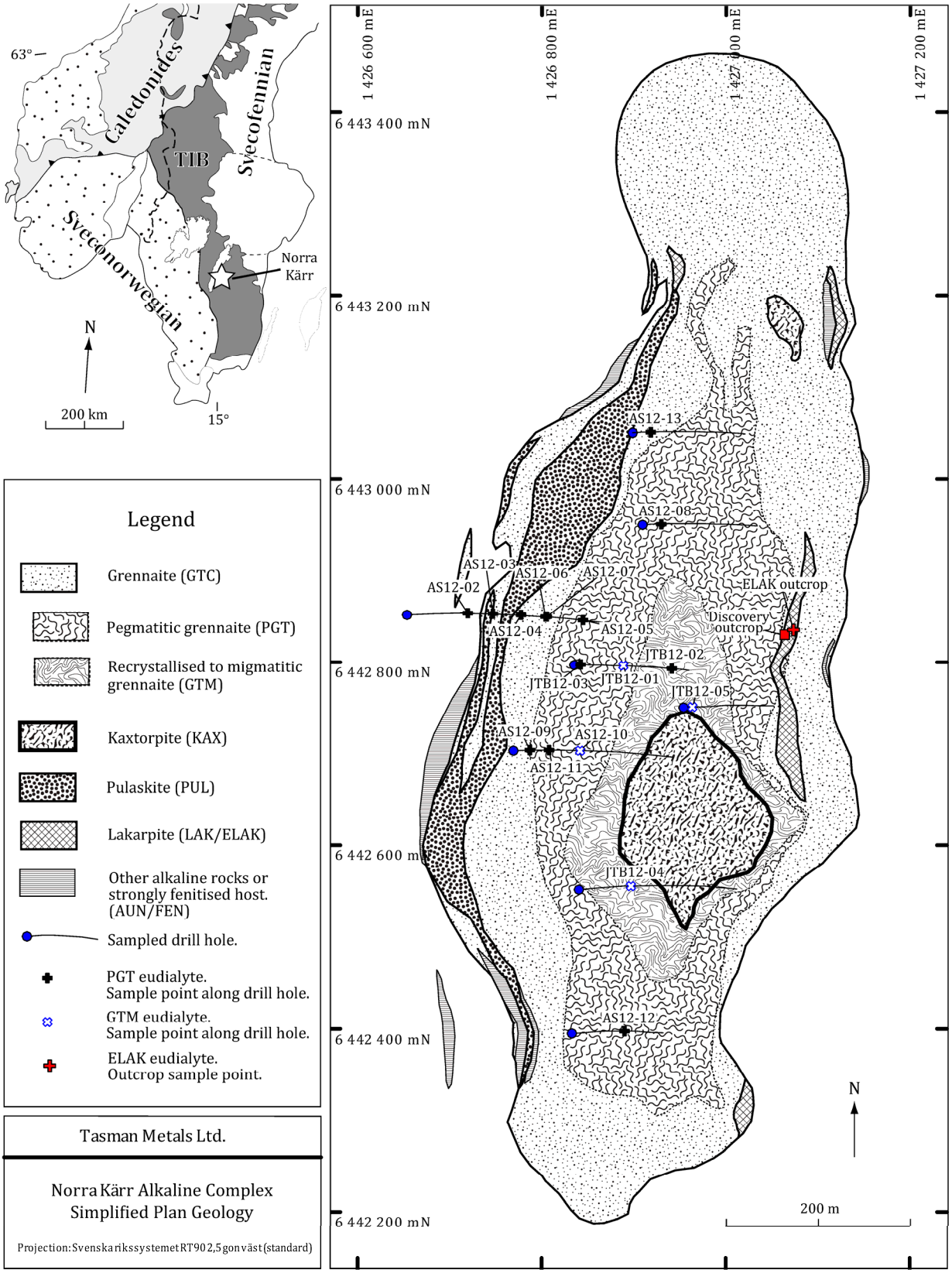

Until recently the age of emplacement of Norra Kärr was not well established, but our U-Pb zircon dating revealed that the related metasomatic alteration of the country rocks (fenitisation), and thus Norra Kärr's magmatism, occurred at 1489 ± 8 Ma [30], which is a refinement of an imprecise whole-rock Rb-Sr age of 1545 ± 61 Ma [31,32]. The complex intruded into 1791 ± 8 Ma granites [33] that belong to the Småland-Värmland granitoids of "Växjö type", part of the Transscandinavian Igneous Belt (TIB) [34].

An in-depth description and evaluation of the geology of the Norra Kärr Alkaline Complex is beyond the scope of this study. The origin and geological development of the complex have been disputed, especially whether the rocks have undergone metamorphism. Adamson [35], whose thesis is the most thorough academic effort, concluded that igneous processes during emplacement of the complex were responsible for the observed textures, which is in line with Törnebohm's early work [27], and was later supported in particular by Von Eckermann [36,37]. The foliated, locally schistose, nature of the rocks was attributed to magmatic flow.

Koark critically opposed to this view [38–40] and questioned some of the evidence put forth by other authors. After detailed petrofabric studies, his conclusion was that the rocks in Norra Kärr had been deformed. Many textures in the Norra Kärr rocks—e.g., gneissosity, folding, shearing, and evidence of anatexis—suggest a metamorphic overprinting of the initially igneous lithology, and Norra Kärr is now regarded in the literature as a metamorphosed agpaitic complex (e.g., [21]).

A detailed re-examination of the geology, magmatic and post-magmatic evolution of Norra Kärr is the subject of future publications. Below follow brief descriptions of the lithological units in Norra Kärr as we understand them today.

1.3.1. Grennaite

The main rock unit (Figure 2) is a mesocratic fine-grained greyish green nepheline syenite with a clear, locally schistose, foliation (Figure 3a). The major minerals are nepheline, microcline, albite, aegirine, and eudialyte (Figure 4a). Catapleiite also occurs, as small platy or large subhedral grains. Porphyroclasts of microcline perthite and aegirine are common in the fine-grained groundmass. This unit was originally named "catapleiite syenite" [27], but was later given the local name "grennaite" after the nearby town of Gränna [35]. This unit, with catapleiite, is called "GTC" for "grennaite with catapleiite" in Tasman Metals' terminology, which we have adopted in this work.

Towards the center of the complex occurs a sub-unit of grennaite that contains leucosomes as lenticles and bands of medium- to coarse-grained nepheline syenite (Figures 2 and 3B). These veins are common throughout the sub-unit and in some exposures they are volumetrically dominant. They occur both in the plane of foliation and as crosscutting veins, commonly displaying comb structure at the contacts to the fine-grained rock. The leucosomes vary in mineralogy, size, and frequency and predominantly comprise nepheline, microcline, albite, aegirine, red to brown eudialyte, and catapleiite (Figure 4B). Zeolites are common secondary minerals after nepheline and their hematite inclusions often give these pegmatitic leucosomes a reddish character. We interpret these veins as leucosomes formed by anatexis of grennaite. Equivalent rocks with agpaitic indices of 1.0–1.2 have in experiments been found to start melting at 250–350 °C (P_{H_2O} = 1030 bar) [41,42]. This unit is named "PGT" for "grennaite with pegmatites" in Tasman Metals' lithologic nomenclature, although the leucosomes are normally not *sensu stricto* pegmatites.

Figure 3. Rock types of the Norra Kärr Alkaline Complex. Scale bars in cm. (**A**) GTC: Grennaite with bluish-grey subhedral catapleiite grains (Cat); (**B**) PGT: Grennaite migmatite with crosscutting leucosome, containing nepheline (Nph) altered by natrolite (Ntr), microcline (Mc), albite (Ab), eudialyte (Eud), and catapleiite (Cat); (**C**) GTM: Folded grennaite with recrystallised texture, red-stained by zeolites (Zeo); (**D**) KAX: Kaxtorpite with microcline augen (Mc), rich in bluish amphibole (Eck) and aegirine (Aeg); (**E**) ELAK: Lakarpite with pink eudialyte (Eud) and yellow mosandrite (Mos) [3]. (Most mineral abbreviations from Whitney and Evans [43].)

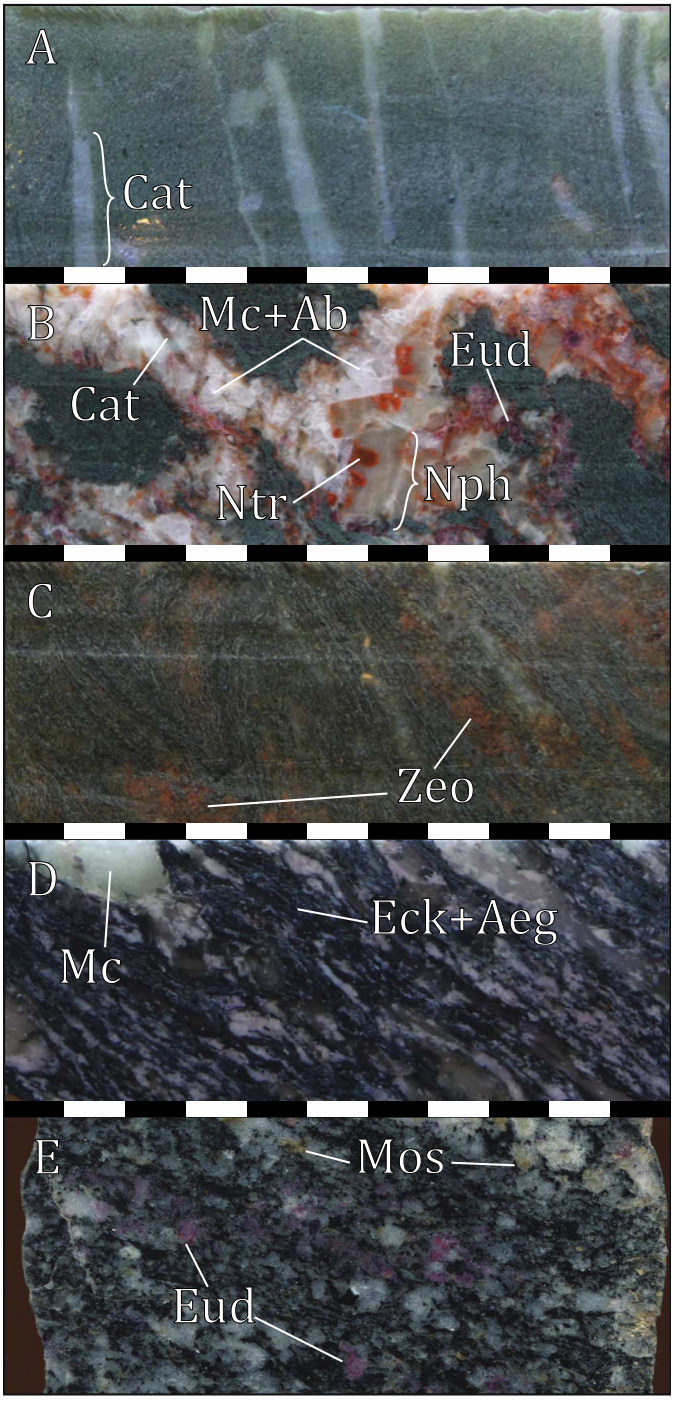

Figure 4. Backscattered electron images of eudialyte-group minerals (EGM) bearing rocks. (**A**) GTC: fine-grained eudialyte (Eud) with aegirine (Aeg), microcline (Mc), nepheline (Nph), and albite (Ab); (**B**) PGT: large eudialyte (Eud) from a coarse-grained leucosome with catapleiite (Cat), aegirine (Aeg), nepheline (Nph), and zeolite (Zeo); (**C**) GTM: eudialyte (Eud) with aegirine (Aeg), microcline (Mc), albite (Ab), and zeolite (Zeo); (**D**) ELAK: eudialyte (Eud) with mosandrite [3] (Mos), arfvedsonite (Arf), microcline (Mc), and albite (Ab). (Most mineral abbreviations from Whitney and Evans [43].)

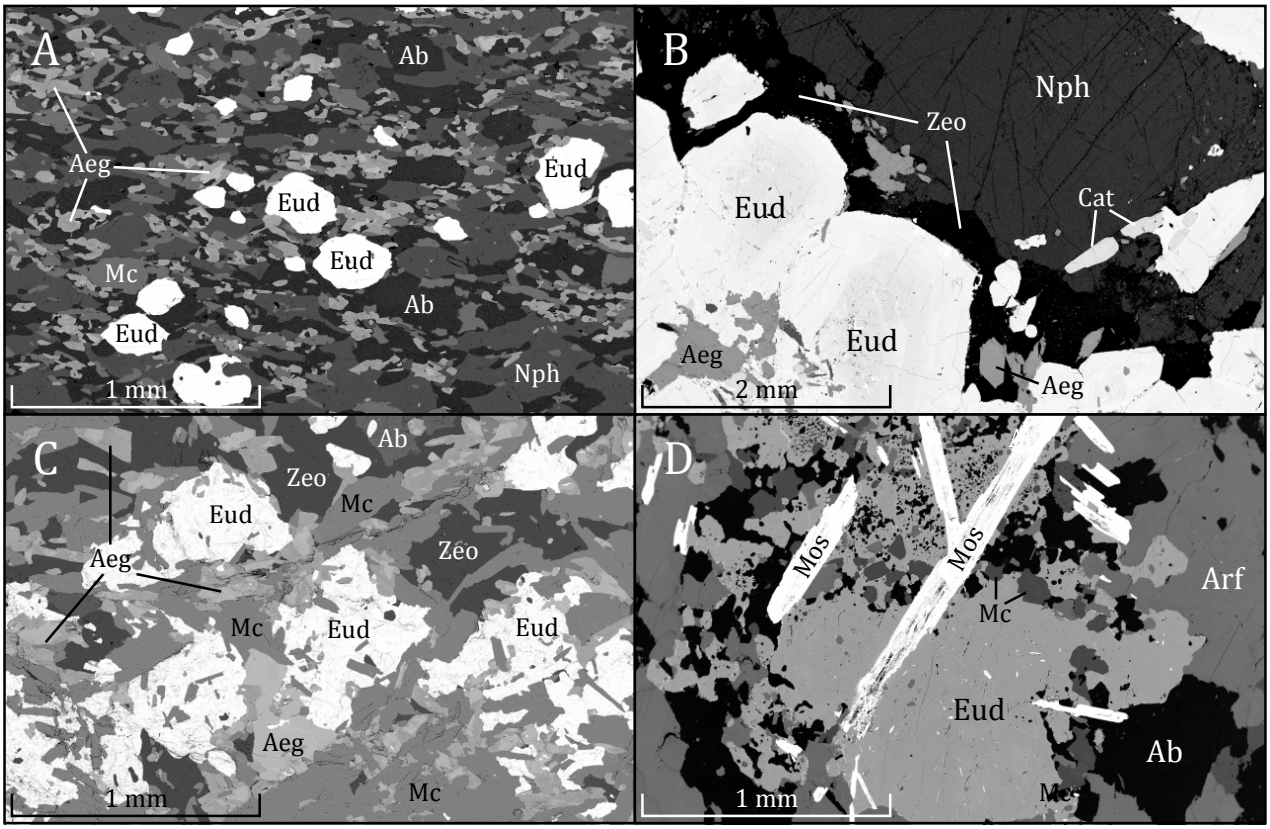

Another variety of grennaite occurs exclusively near the center of the complex (Figures 2 and 3C). It is composed of the same minerals as the other types (Figure 4C), but zeolites are more common and pectolite occurs as a minor phase. GTM differs from the other grennaites both in texture and chemical composition. The rock is commonly tightly folded, has a paler color, and generally exhibits a recrystallized or slightly migmatitic texture. This unit is named "GTM" for "migmatitic grennaite" in Tasman Metals' lithologic nomenclature.

1.3.2. Kaxtorpite

"Kaxtorpite" occurs at the center of the complex and is a melanocratic nepheline syenite, which is a foliated and commonly folded rock (Figures 2 and 3D). The rock type was named after the farm Kaxtorp [35]. It is made up mainly of nepheline, microcline, albite, eckermannite, aegirine, and catapleiite.

Pectolite and lorenzenite occur frequently, as well as secondary zeolite minerals. Willemite—normally a secondary mineral after sphalerite—is an accessory mineral in the kaxtorpite, but sphalerite has at present not been identified in this unit, although it has been observed elsewhere.

1.3.3. Lakarpite

Törnebohm [27] described a rock type from the northern parts of the complex, in which he identified rosenbuschite, and named it "lakarpite" after the nearby farm Lakarp (Figure 2). He regarded the rock as a diorite, however Adamson [35] claimed that nepheline also is present in the rock. This rock is a mesocratic nepheline syenite that is mainly composed of albite, arfvedsonite, and nepheline with microcline, rosenbuschite, mosandrite [3], apatite, titanite, and abundant fluorite [35]. It does not—as far as observed in this study—contain eudialyte.

Another type of lakarpite is found near the eastern boundary of the complex, usually in or near the transition from the PGT to the GTC domain. This rock is generally mafic and is made up of arfvedsonite and aegirine, microcline, albite, nepheline, pectolite, pink eudialyte, mosandrite [3], and fluorite (Figures 3E and 4D). This unit, with pink eudialyte, is named "ELAK" for "lakarpite with eudialyte" in Tasman Metals' lithologic nomenclature. The "Discovery outcrop", which is rich in pink eudialyte (Figure 1), is located in the contact zone between the PGT and ELAK domains (Figure 2).

Lakarpite mainly has lower concentrations of MgO and CaO than kaxtorpite and is richer in ZrO_2. Lakarpite generally has a more massive texture than kaxtorpite.

1.3.4. Pulaskite

Pulaskite (*i.e.*, an alkali feldspar syenite with only minor nepheline [6]) has been described by previous authors [31,35] and is the only rock type in Norra Kärr that has been given a common petrographic name. It is not clear to us whether pulaskite occurs as a distinct rock type, but we are confident that if it does it is intimately related to the rosenbuschite-bearing northern lakarpite.

The petrogenetic and structural relationships between the main rock type—the grennaite—and the other rock types—the kaxtorpite, varieties of lakarpite, and possible pulaskite—are today still not well understood.

Surrounding the Norra Kärr Alkaline Complex is a heterogeneous aureole in which the host granitoids were affected by alkali metasomatism (fenitisation). The thickness of the metasomatised zone is 25–100 m wide [35].

1.4. Exploration History

The Swedish mining company Boliden AB prospected and test mined in Norra Kärr during and after the Second World War. The main target was zirconium at a time when Sweden was developing nuclear energy. Nepheline and feldspar also had potential for use in glass and ceramics [44].

In 1948 Boliden signed an agreement with the landowners, allowing them to mine the site. During the spring of 1949 several test pits were sunk and attempts were made to separate nepheline and feldspar from aegirine, which proved to be difficult. Meanwhile, other zirconium deposits were being explored, in particular Brazilian zircon deposits, and Boliden soon put the Norra Kärr project on hold [44].

Boliden made another unsuccessful attempt at extracting nepheline, zirconium, and hafnium in 1974. In the 1990s Boliden put the land up for sale and gave up their exploration claim completely in 2001 [44].

Renewed interest in the economic potential of Norra Kärr has existed since Tasman Metals Ltd. began exploration for rare-earth elements in the fall of 2009 [45]. The primary ore mineral is eudialyte.

2. Methods

Eudialyte-rich samples were collected from Tasman's drill cores in 17 different places with the addition of one sample that was collected in the field (see Table 4 and Figure 2). Most samples were taken roughly 50 m apart to form vertical sections through the Norra Kärr complex and to represent the different units of the deposit. Tasman's cores were drilled at a 50° dip angle to the east. Please note that the drill hole and sample locations in Figure 2 are projected to the surface.

Table 4. List of the eudialyte samples that were taken for this study.

Sample	Core	Depth (m)	Tasman Unit
AS12-01	*Field Sample* [1]	0	ELAK
AS12-02	NKA12062	106.5	PGT
AS12-03	NKA12062	146.5	PGT
AS12-04	NKA12062	198.5	PGT
AS12-05	NKA12062	299.9	PGT
AS12-06	NKA12062	251.5	PGT
AS12-07	NKA12062	252.5	PGT
AS12-08	NKA12067	30.8	PGT
AS12-09	NKA11039	27.0	PGT
AS12-10	NKA11039	113.0	GTM
AS12-11	NKA11039	62.0	PGT
AS12-12	NKA10011	89.3	PGT
AS12-13	NKA12069	28.8	PGT
JTB12-01	NQ12004	71.5	GTM
JTB12-02	NQ12004	158.4	PGT
JTB12-03	NQ12004	12.5	PGT
JTB12-04	NKA12075	90.4	GTM
JTB12-05	NKA12071	16.3	GTM

Note: [1] 58°6.201' N, 14°34.091' E: lakarpite outcrop with eudialyte.

The samples were manually crushed and roughly ten eudialyte grains per sample were picked and mounted under a binocular microscope and cast into an epoxy puck, which was ground and polished with three micron diamond slurry.

2.1. Whole-Rock Composition

Tasman's drill cores were analyzed by ALS Minerals ultra-trace level method ME-MS81. In this procedure 0.2 g of sample was decomposed with 0.9 g lithium metaborate flux in an oven at 1000 °C. The fused sample was then dissolved in 100 mL solution of 4% HNO_3 and 2% HCl and analyzed by ICP-MS. Elements that are included in the ME-MS81 package are Ag, Ba, Ce, Co, Cr, Cs, Cu, Dy, Er, Eu, Ga, Gd, Hf, Ho, La, Lu, Mo, Nb, Nd, Ni, Pb, Pr, Rb, Sm, Sn, Sr, Ta, Tb, Th, Tl, Tm, U, V, W, Y, Yb, Zn, and Zr [46]. ALS disclaimer: "Some base metal oxides and sulphides may not be completely decomposed by the lithium borate fusion. Results for Ag, Co, Cu, Mo, Ni, Pb, and Zn will not likely be quantitative by this method." Analyses in which the Zr concentration exceeded 10,000 ppm were additionally analyzed by X-ray fluorescence (XRF) method ME-XRF10.

Whole-rock major element analyses of representative samples of different units were also made by ALS Minerals using method ME-MS81d, which includes the above methods, complemented by Al_2O_3, BaO, CaO, Cr_2O_3, Fe_2O_3, MgO, MnO, P_2O_5, K_2O, SiO_2, Na_2O, SrO, and TiO_2 by ICP-AES [47].

Agpaitic indices (A.I.) for the whole-rock analyses were calculated as the molar proportions of (Na + K)/Al and are presented in Table 5.

2.2. Electron Microprobe Analysis by Wavelength Dispersive X-Ray Spectrometry (WDS-EMP)

WDS-EMP analyses were done on a Cameca SX100 (CAMECA SAS, Gennevilliers, France) with 5 wavelength-dispersive spectrometers at the Department of Geosciences, University of Oslo. Accelerating voltage 15 kV, beam current 15 nA, and beam size 10 μm were used for analysis of eudialyte. Na, Cl, and K were analyzed first to avoid loss due to electron damage. Calibration standards and X-ray lines used were wollastonite (Si Kα, Ca Kα), Al_2O_3 (Al Kα), pyrophanite (Ti Kα, Mn Kα), Fe metal (Fe Kα), orthoclase (K Kα), albite (Na Kα), synthetic alforsite (Cl Kα), Monastery Mine zircon (Zr Lα), Nb metal (Nb Lα), synthetic orthophosphates [48] for REE and Y (La Lα, Ce Lα, Nd Lβ, Y Lα), and Hf metal (Hf Mα). Matrix corrections were done according to the PAP procedure [49]. Peak counting times of 10 s were used for Si, Ca, K, and Na and 20 s for all other elements except Nd (30 s) and total backgrounds equaled the peak counting time. Pulse height discrimination was used to minimize interferences from higher order X-ray lines. Analyses are given in Table 6, with typical analytical uncertainties (2σ) and detection limits.

2.3. Scanning Electron Microscopy by Energy Dispersive Spectrometry (SEM-EDS)

SEM-EDS analyses were done with a Hitachi (Tokyo, Japan) S-4300N scanning electron microscrope fitted with an Oxford Instruments (Oxford, UK) INCA EDS system at the Department of Earth Sciences, University of Gothenburg. The SEM was operated at high vacuum with accelerating voltage 20 kV and specimen current 3.5 nA. A Co metal standard linked to the calibration standards was used for quantitative calibration. Tests were done with a focused electron beam and longer live times (up to 5000 s), but this resulted in severe decomposition of the mineral under the beam and loss of Na. Eudialytes were thus analyzed by selecting rectangular areas of approximately 500–2500 μm^2, rather than spot analyses. Each analysis with 360 s live time took about 10 min, whereas WDS-EMP analyses took about 6 min. Data reduction was done by Oxford INCA software using the XPP (based on Phi-Rho-Z) matrix correction procedure.

The calibration standards were, unless otherwise specified, manufactured by Microanalysis Consultants, St. Ives, Cambridgeshire, UK [50]. The standards are jadeite (Na), wollastonite (Si and Ca), tugtupite (Cl: SPI Supplies, West Chester, PA, USA [51]), orthoclase (K), rutile (Ti), Mn metal (Mn), Fe metal (Fe), Zr metal (Zr; SPI), Nb metal (Nb), REE glasses for each element including Y (REE), and Hf metal (Hf). Na, Si, Cl, K, Ca, Ti, Mn, Fe, and Y were quantified using the K-lines, whereas Zr, Nb, REE, and Hf used the L-lines.

Analyses with typical uncertainties (2σ) and detection limits are given in Table 7. Detection limits are thrice the 1σ uncertainty at low concentration; e.g., 0.14 wt % for Ce_2O_3, 0.03 wt % for K_2O.

3. Results

3.1. Whole-Rock Composition

Table 5 presents whole-rock major and trace element analyses of representative samples of the main rock types at Norra Kärr, from the exploration drilling by Tasman. These whole-rock analyses constitute the geochemical context that is relevant for our own eudialyte analyses from the equivalent rock types.

Table 5. Whole-rock analyses of representative samples of the different rock types. The agpaitic index (A.I.) is described in Section 1.1.

	Grennaite			Kaxtorpite	Lakarpite
Sample	**GTC 400269**	**PGT 407497**	**GTM 407575**	**KAX 401205**	**ELAK 407810**
	wt %	**wt %**	**wt %**	**wt %**	**wt %**
SiO_2	57.13	55.10	55.30	57.67	59.80
TiO_2	0.01	0.08	0.08	0.56	0.06
ZrO_2	1.58	2.23	1.35	0.098	1.61
Al_2O_3	19.46	16.65	17.50	15.46	14.30
Fe_2O_3	4.41	6.51	4.88	4.59	6.49
MnO	0.12	0.40	0.38	0.86	0.31
MgO	0.01	0.11	0.09	1.70	0.24
CaO	0.55	1.73	1.57	4.37	1.66
Na_2O	11.59	12.45	9.81	8.53	10.15
K_2O	3.63	2.47	3.59	3.28	3.85
P_2O_5	0.008	0.02	0.01	0.008	b.d.l.
L.O.I.	1.38	3.03	3.95	2.29	1.58
Total	98.31	98.58	97.19	99.45	98.46
A.I.	1.18	1.39	1.14	1.14	1.46
	ppm	**ppm**	**ppm**	**ppm**	**ppm**
V	b.d.l.	9	b.d.l.	58	19
Cr	b.d.l.	50	40	60	30
Co	b.d.l.	b.d.l.	1.8	9.1	0.9
Ni	b.d.l.	b.d.l.	b.d.l.	5	b.d.l.
Cu	b.d.l.	b.d.l.	b.d.l.	15	b.d.l.
Zn	124	98	173	1695	172
Ga	86.9	91.1	110.5	62.8	56.4
Rb	272	203	514	237	290
Sr	25.7	182.5	162	350	105.5
Y	816	3590	1080	168.5	1895
Nb	203	909	213	64.4	447
Mo	b.d.l.	b.d.l.	b.d.l.	b.d.l.	b.d.l.
Ag	b.d.l.	b.d.l.	b.d.l.	b.d.l.	1
Sn	52	144	112	21	77
Cs	4.05	4.21	18	13.35	1.73
Ba	n.a.	43.6	81.5	n.a.	134.5
La	206	873	585	123.5	448
Ce	411	2020	1045	200	995

Table 5. *Cont.*

Sample	Grennaite			Kaxtorpite	Lakarpite
	GTC 400269	PGT 407497	GTM 407575	KAX 401205	ELAK 407810
	ppm	ppm	ppm	ppm	ppm
Pr	59	263	118	24	137
Nd	237	1140	409	87.1	574
Sm	67	328	90.4	19	167.5
Eu	10	38.2	10.55	3	17.05
Gd	82	359	98.8	22	165
Tb	19.35	69.2	20.2	3.67	36.6
Dy	144	453	144.5	25	249
Ho	35	105	36.3	5	61.4
Er	112	305	112.5	16	189.5
Tm	18	45.7	17.8	2	30
Yb	113.5	301	118	15.25	179.5
Lu	16.3	37.9	15.65	2.09	25.2
Hf	302	349	240	15.6	301
Ta	21.9	45.9	18.7	1.9	36.8
W	3	6	1	b.d.l.	4
Tl	1.1	1.3	1.3	1	0.5
Pb	168	182	245	249	44
Th	6.11	4.95	9.22	20	9.02
U	5.31	7.36	22.7	9.54	4.99
TREO + Y_2O_3 [1]	0.281	1.193	0.466	0.085	0.621
HREO + Y_2O_3 [2]	59.2%	54.7%	43.6%	37.7%	56.3%

Notes: b.d.l.: below detection limit; n.a.: not analyzed; [1] Weight percent total rare-earth oxide (TREO) including yttrium oxide; [2] Percent heavy rare-earth oxide (HREO; Eu–Lu) plus yttrium oxide of TREO + Y_2O_3.

All of the analyzed rock types are agpaitic, following the mineralogical definition of Sørensen [5]. Striking features of the analyses are the high concentrations of alkali elements, alumina, and zirconia. In view of the generally accepted origin by differentiation of alkali basalt [1] (in the case of a negative Eu anomaly), the very low Ca, Mg, and Ti concentrations require extreme crystal fractionation.

The economic potential of these rocks is illustrated by their high REE and zirconia contents. Both light and heavy REE clearly acted incompatibly during fractionation, with the exception of Eu, which is compatible as Eu^{2+} in plagioclase. The economically beneficial low Th and U contents probably reflect removal by fractionation of apatite.

3.2. Electron Microprobe Analysis by Wavelength Dispersive X-Ray Spectrometry (WDS-EMP)

WDS-EMP results that are used in direct comparisons with SEM-EDS results in this article are presented in Table 6. For a complete list of WDS-EMP analyses used in this study see Electronic Appendix 1. The analysis labels (e.g., #69) represent the WDS-EMP analysis spot number for individual eudialyte grains. Typical uncertainties (2σ) and detection limits are presented in the last column.

Table 6. Analyses of eudialyte-group minerals by Wavelength Dispersive X-ray Spectrometry (WDS-EMP).

Sample	#69	#9	#16	#20	#87	Typical errors
	AS12-01	AS12-02	AS12-03	AS12-04	AS12-05	2σ
	wt %	wt %	wt %	wt %	wt %	wt %
SiO_2	49.83	47.76	47.46	47.98	47.94	0.43
Al_2O_3	0.13	0.32	0.26	0.27	0.23	0.02
Nb_2O_5	b.d.l.	0.60	0.92	0.56	0.94	0.17
ZrO_2	11.91	11.91	11.94	11.71	11.61	0.23
HfO_2	0.22	0.37	0.36	0.23	0.35	0.04
TiO_2	0.18	0.14	0.10	0.13	0.08	0.03
La_2O_3	0.12	0.42	0.61	0.60	0.63	0.09
Ce_2O_3	0.16	1.15	1.36	1.77	1.27	0.15
Nd_2O_3	b.d.l.	0.81	0.70	1.00	0.65	0.15
Y_2O_3	0.50	3.14	3.01	3.04	3.18	0.09
FeO	5.47	3.07	3.07	3.03	2.51	0.09
MnO	1.45	1.95	2.20	2.24	2.49	0.08
CaO	10.40	7.79	7.16	6.79	7.95	0.24
Na_2O	13.04	14.06	13.74	13.98	12.19	0.42
K_2O	0.39	0.57	0.45	0.35	0.41	0.04
Cl	0.46	0.41	0.50	0.41	0.48	0.04
Total	94.15	94.29	93.62	93.92	92.72	-
Sample	**#148**	**#113**	**#147**	**#91**	**#104**	**Detection limits**
	JTB12-05	**JTB12-04**	**JTB12-05**	**AS12-06**	**AS12-10**	
	wt %	**wt %**	**wt %**	**wt %**	**wt %**	**wt %**
SiO_2	48.16	48.18	48.48	47.73	48.42	0.08
Al_2O_3	0.25	0.12	0.09	0.30	0.19	0.03
Nb_2O_5	0.48	0.44	1.01	0.79	0.48	0.3
ZrO_2	11.70	11.22	11.50	12.44	11.50	0.10
HfO_2	0.19	0.32	0.35	0.33	0.28	0.09
TiO_2	0.05	0.20	0.18	0.12	0.18	0.03
La_2O_3	0.90	0.88	1.72	0.65	1.28	0.2
Ce_2O_3	2.18	2.14	2.68	1.47	2.79	0.2
Nd_2O_3	1.38	1.07	0.93	0.71	1.31	0.2
Y_2O_3	2.25	3.42	1.64	2.76	2.27	0.06
FeO	3.10	0.83	1.24	2.78	0.91	0.08
MnO	2.72	3.10	4.35	2.17	5.36	0.08
CaO	6.72	6.79	7.24	7.33	5.19	0.08
Na_2O	12.47	8.53	8.98	12.37	11.13	0.08
K_2O	0.67	1.06	0.91	0.52	0.59	0.03
Cl	0.24	0.29	0.20	0.40	0.41	0.02
Total	93.24	88.44	91.31	92.67	92.09	-

Note: b.d.l.: below detection limit.

3.3. Scanning Electron Microscopy by Energy Dispersive Spectrometry (SEM-EDS)

Analyses of eudialyte-group minerals by SEM-EDS that are used in direct comparisons to WDS-EMP analyses in this article are presented in Table 7. The analysis labels (e.g., #69) represents the corresponding WDS-EMP analysis spot numbers for individual eudialyte grains. The last column presents typical uncertainties (2σ). Analysis pairs #113a and #113b as well as #147a and #147b are both compared to the same WDS-EMP analyses (#113 and #147) due to heterogeneity in those respective eudialyte grains.

Table 7. Analyses of eudialyte-group minerals by Scanning Electron Microscopy by Energy Dispersive Spectrometry (SEM-EDS).

	#69	**#9**	**#16**	**#20**	**#87**	**#148**	**Typical errors**
Sample	**AS12-01**	**AS12-02**	**AS12-03**	**AS12-04**	**AS12-05**	**JTB12-05**	**2σ**
	wt %	**wt %**	**wt %**	**wt %**	**wt %**	**wt %**	**wt %**
SiO_2	49.88	47.41	47.41	48.39	48.16	48.08	0.17
Al_2O_3	n.a.	n.a.	n.a.	n.a.	n.a.	n.a.	-
Nb_2O_5	0.56	1.22	1.12	1.00	1.33	0.94	0.14
ZrO_2	11.94	11.99	11.89	12.25	12.06	11.99	0.22
HfO_2	0.30	0.23	0.23	0.47	0.32	b.d.l.	0.14
TiO_2	0.17	0.13	0.09	0.28	0.06	0.07	0.03
La_2O_3	b.d.l.	0.53	0.57	0.56	0.48	0.64	0.09
Ce_2O_3	b.d.l.	1.09	1.23	1.37	1.11	1.98	0.09
Pr_2O_3	b.d.l.	b.d.l.	0.17	0.25	0.21	0.25	0.09
Nd_2O_3	b.d.l.	0.67	0.65	1.22	0.67	1.19	0.09
Sm_2O_3	b.d.l.	0.20	0.23	0.40	0.20	0.25	0.09
Eu_2O_3	b.d.l.	b.d.l.	b.d.l.	b.d.l.	b.d.l.	b.d.l.	0.16
Gd_2O_3	b.d.l.	0.28	0.26	b.d.l.	0.39	b.d.l.	0.16
Tb_2O_3	b.d.l.	b.d.l.	b.d.l.	b.d.l.	b.d.l.	b.d.l.	0.16
Dy_2O_3	b.d.l.	0.46	0.48	b.d.l.	0.62	0.31	0.16
Ho_2O_3	b.d.l.	b.d.l.	b.d.l.	b.d.l.	b.d.l.	b.d.l.	0.11
Er_2O_3	b.d.l.	0.33	0.37	b.d.l.	0.30	b.d.l.	0.14
Tm_2O_3	b.d.l.	b.d.l.	b.d.l.	b.d.l.	b.d.l.	b.d.l.	0.11
Yb_2O_3	b.d.l.	0.34	b.d.l.	b.d.l.	0.21	b.d.l.	0.11
Lu_2O_3	b.d.l.	b.d.l.	b.d.l.	b.d.l.	b.d.l.	b.d.l.	0.11
Y_2O_3	b.d.l.	3.02	3.00	3.97	2.89	2.38	0.69
FeO	5.54	3.05	3.16	3.00	2.54	3.21	0.08
MnO	1.42	2.00	1.98	2.22	2.41	2.60	0.08
CaO	10.76	7.87	7.43	6.92	7.98	6.67	0.06
Na_2O	11.83	13.21	13.36	14.00	11.67	12.09	0.32
K_2O	0.43	0.51	0.44	0.29	0.35	0.64	0.02
Cl	0.44	0.39	0.50	0.37	0.46	0.22	0.02
Total	93.76	93.24	92.99	96.24	92.40	92.84	-

Table 7. *Cont.*

Sample	#113a JTB12-04 wt %	#113b JTB12-04 wt %	#147a JTB12-05 wt %	#147b JTB12-05 wt %	#91 AS12-06 wt %	#104 AS12-10 wt %	Detection limits wt %
SiO_2	49.24	48.55	47.98	47.51	47.92	48.14	0.26
Al_2O_3	n.a.	n.a.	n.a.	n.a.	n.a.	n.a.	-
Nb_2O_5	0.63	0.60	1.74	1.82	0.93	0.85	0.21
ZrO_2	11.87	11.93	11.40	11.32	12.27	11.92	0.33
HfO_2	0.34	0.24	0.21	0.23	0.23	0.24	0.21
TiO_2	0.21	0.17	0.18	0.17	0.17	0.17	0.05
La_2O_3	0.76	0.72	1.67	1.90	0.61	1.00	0.14
Ce_2O_3	1.97	2.07	2.58	2.66	1.41	2.59	0.14
Pr_2O_3	0.16	0.30	0.28	0.17	0.15	0.31	0.14
Nd_2O_3	1.01	1.10	0.82	0.78	0.77	1.18	0.14
Sm_2O_3	0.32	0.21	0.25	b.d.l.	0.22	0.23	0.14
Eu_2O_3	b.d.l.	b.d.l.	b.d.l.	b.d.l.	b.d.l.	b.d.l.	0.24
Gd_2O_3	0.36	b.d.l.	0.36	b.d.l.	b.d.l.	0.33	0.24
Tb_2O_3	b.d.l.	b.d.l.	b.d.l.	b.d.l.	b.d.l.	b.d.l.	0.24
Dy_2O_3	0.44	0.43	b.d.l.	0.24	0.30	0.31	0.24
Ho_2O_3	b.d.l.	b.d.l.	b.d.l.	b.d.l.	b.d.l.	b.d.l.	0.17
Er_2O_3	0.31	b.d.l.	b.d.l.	b.d.l.	0.29	0.20	0.21
Tm_2O_3	b.d.l.	b.d.l.	b.d.l.	b.d.l.	b.d.l.	b.d.l.	0.17
Yb_2O_3	0.27	b.d.l.	b.d.l.	b.d.l.	0.24	0.19	0.17
Lu_2O_3	b.d.l.	b.d.l.	b.d.l.	b.d.l.	b.d.l.	b.d.l.	0.17
Y_2O_3	2.56	3.26	1.82	1.35	2.81	1.96	1.04
FeO	1.09	1.04	1.31	1.19	2.92	1.00	0.12
MnO	3.11	3.08	4.57	4.60	2.11	5.06	0.12
CaO	6.58	6.45	7.34	7.40	7.49	5.14	0.09
Na_2O	7.90	8.07	9.05	8.19	12.12	10.84	0.48
K_2O	0.99	0.99	0.81	0.83	0.53	0.58	0.03
Cl	0.22	0.17	0.17	0.16	0.39	0.35	0.03
Total	88.44	88.40	91.54	89.99	92.62	90.96	-

Notes: n.a.: not analyzed; b.d.l.: below detection limit.

4. Discussion

We will first discuss our approach for quantifying the SEM-EDS analyses, then move on to compare the analyses by WDS-EMP and SEM-EDS. Finally we discuss the petrogenetic implications of eudialyte-group minerals for the Norra Kärr Alkaline Complex.

4.1. Processing of SEM-EDS Spectra

The quality of an EDS analysis depends very much on the appropriate elements being added into the peak-stripping menu. For instance, quantifying an EDS analysis of the mineral plagioclase without including Na will result in a faulty value for Ca, because the correction factors are based on the entire composition. For eudialyte analyses the effects of K- and L-line overlaps present some challenges.

Our approach to optimize the set-up for doing sound eudialyte analyses began by manually adding all the essential main elements (e.g., Na, Si, Ca, Zr) along with possible minor elements (e.g., Ti, Ba, Ta, Th). The valency of Fe was set to 2+ and oxygen was calculated stoichiometrically. We then took one analysis and attempted to identify interferences in the quantification.

Initially, the Al concentration was 1.33% (element), but varied between different analyses. Removing Yb (0.17%) from the menu brought Al down to 0.76% and removing Tm, Yb, and Lu resulted in a value of 0.02% for Al, which is below the detection limit ($3\sigma = 0.03\%$). Our conclusion is that including Tm, Yb, and Lu results in a too-large M-series subtraction, which removes the background for Al and gives too high Al concentrations. Since Al could not be detected and we are interested in REE, we decided to remove Al from the menu, which has no significant effect on the correction procedure.

Zr was originally quantified by using the K-line, which gave a zirconia concentration of 14.3%. The Zr Kα line is close to the upper limit of the EDS spectrum at an operating voltage of 20 kV and has much lower intensity than Lα. Zr was changed to the higher-intensity L-line, which gave 12.4%, more in accordance with WDS-EMP analyses, suggesting that the peak-stripping procedure worked well.

Originally, Ta was included in the menu, because eudialyte-group minerals may incorporate Ta in detectable quantities [19]. Ta was quantified on the M-series to 1.34%, however a peak search on WDS came up with no clear Ta peak. We concluded that Ta was probably falsely quantified from Y and Si K-series peaks. Changing Ta quantification to the L-line instead resulted in a value below the detection limit (−0.01%), which also suggests that there is no significant amount of Ta.

4.2. Comparing SEM-EDS and WDS-EMP

Energy-dispersive (EDS) and wavelength-dispersive spectrometry (WDS) use different approaches to quantify the chemistry of an X-ray analysis. WDS determines concentrations based on a peak count at a specific wavelength and subtracts average background counts from both sides of the peak, whereas EDS has much broader peaks and the analysis is based on peak stripping, using profiles for each element, from the entire energy-dispersive spectrum.

WDS requires expertise to set up correctly, to avoid interfering peaks and also the choice of optimal spectrometer crystals to each element. The WDS software can assign peaks automatically, but blind trust in such software often leads to semi-quantitative analyses. WDS-EMP also requires a few hours of calibration on standards prior to every analytical session.

EDS is in practice more straightforward and user-friendly and the software can often automatically deconvolute overlapping peaks for the present elements. However, to correctly analyze a mineral as complex as the eudialyte group the software needs significant help from the operator as detailed above. Interferences tend to be more problematic on EDS and can sometimes not be resolved.

Figure 5 graphically presents statistic comparisons of analyses on the same spot of respective eudialyte grains by both SEM-EDS and WDS-EMP, using analytical results from Tables 6 and 7. Rectangles in the top left corners of the diagrams represent 2σ analytical uncertainties of the two methods. The theoretical 1:1 ratio—*i.e.*, perfect correlation—is shown as a grey dashed line. For SiO_2 and ZrO_2 relative 2% deviations from the ideal correlation are given by black dashed lines. Trend lines for the calculated correlations are shown in blue. Formulae for the trend lines (shown in Figure 5) were

calculated by assuming a simple linear model, $y = ax + b$ where a represents the ratio factor between y (WDS-EMP) and x (SEM-EDS) the intercept b was set to 0. The value for goodness of fit or coefficient of determination, R^2, (also shown in Figure 5) can be used to test how significant the simple linear model is for the respective data. The closer the value for R^2 is to 1, the more valid the linear model is.

Figure 5. Comparisons of analyses in weight percent oxide by SEM-EDS and WDS-EMP on the same spot of respective eudialyte grains. Trend lines are shown in blue. The theoretical 1:1 ratio is shown as a grey dashed line. Rectangles in the top left corner of each diagram represent 2σ analytical uncertainties for both methods. Formulae for the trend lines are shown as $y = ax + b$; where a represents the factor difference between the two analytical methods, the intercept b was set to 0. The goodness of fit, R^2, in essence shows how well the simple linear model fits the data.

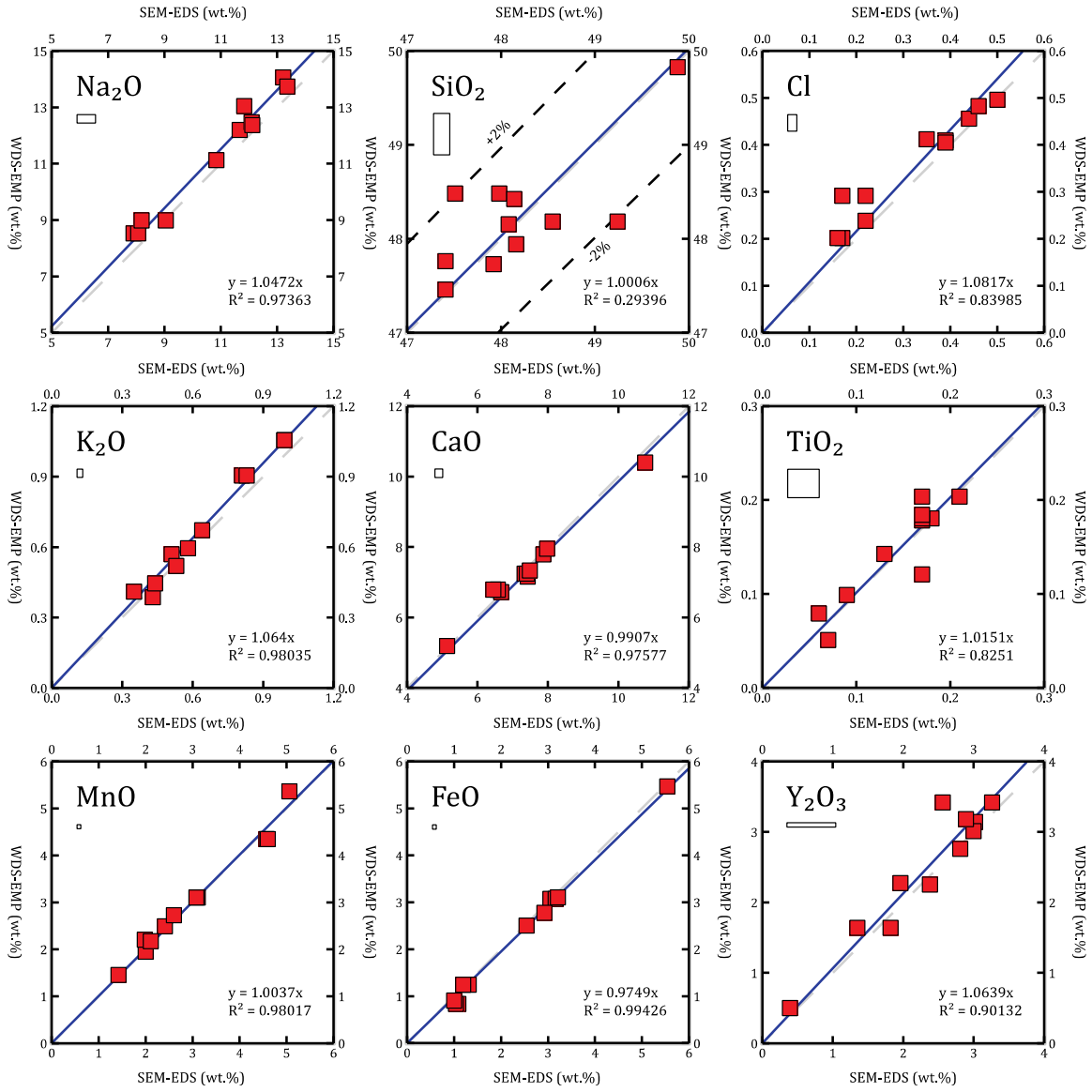

Figure 5. *Cont.*

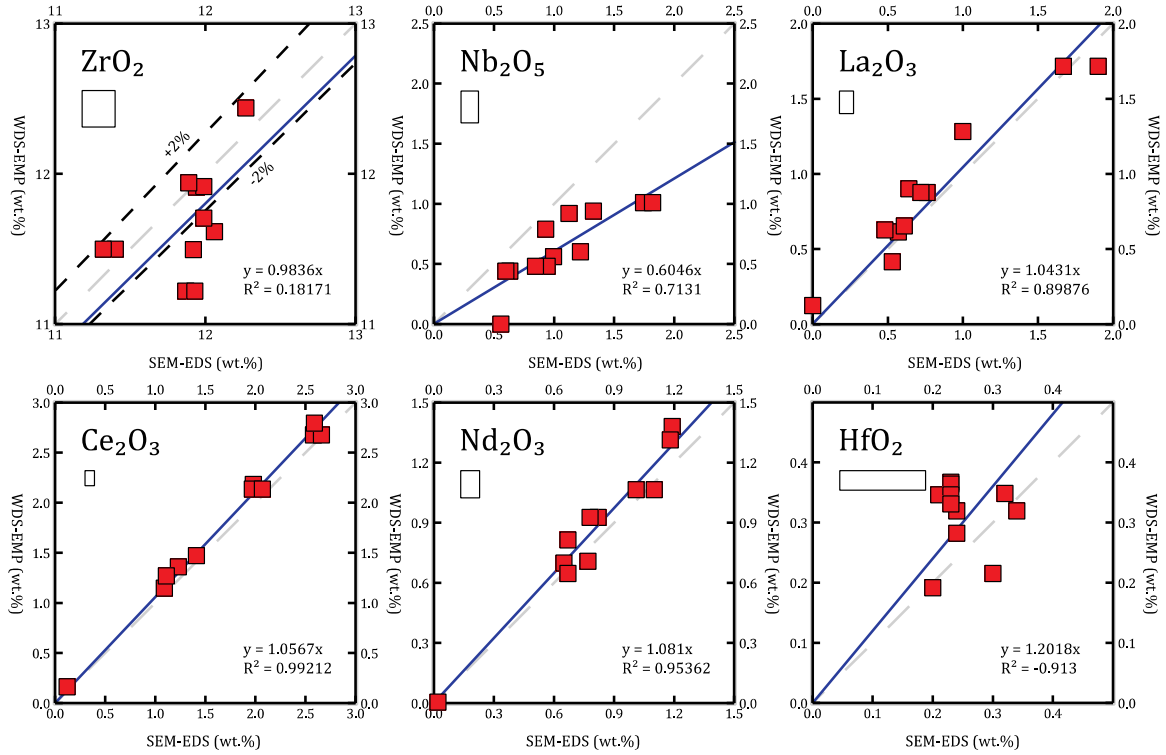

If $a = 1$, then $y = x$ which in words means that SEM-EDS and WDS-EMP gave exactly the same result. If $a = 0.5$, then $y = 0.5x$, which means that the result from WDS-EMP is exactly half of the result from SEM-EDS. Theoretically this implies that either the SEM-EDS value is too high or the WDS-EMP value is too low.

Basically, if $R^2 = 1$, then 100% of the variation in the data is explained by the linear model. If $R^2 = 0.9$ then 90% of the variation in the data is explained by the linear model and the remaining 10% is controlled by an unknown. Thus, if both methods would correlate perfectly, then $a = 1$and $R^2 = 1$.

Based on this comparison, we argue that even for a mineral as complex as eudialyte, with the proper calibration and set-up, results produced by SEM-EDS are close to those produced by WDS-EMP. Due to the good correlation, we feel particularly confident about results for Na, Cl, K, Ca, Ti, Mn, Fe, Y, La, Ce, and Nd, but less confident about Si, Zr, and Hf. There is a clear mismatch between Nb results and Al was not analyzed by EDS. The Si Kα and Zr Lα lines overlap Nb Lα in the EDS spectrum, whereas they are very distinct on a WDS spectrum and are thus theoretically better by WDS.

Most scanning electron microscopes have an energy-dispersive spectrometer and considering the user-friendliness of EDS, this gives an important and readily available tool for reconnaissance work, preliminary analyses in research, and especially in exploration-related studies

4.3. Niobium on WDS-EMP

Based on the comparison above, evidently there is a problem with the analytical results for Nb. They are either too high on SEM-EDS or too low on WDS-EMP (or both).

On the EDS spectrum the Nb Lα line lies close together with Si Kα and Zr Lα, which could potentially result in overestimated values for Nb. However we have not been able to identify significant interferences, following the same kind of procedure as described in Section 4.1.

Eudialyte analyses by WDS-EMP produced negative Nb values in some cases. Not only eudialyte was analyzed during the WDS-EMP session; also a few grains of catapleiite were analyzed. Catapleiite is richer in Zr than eudialyte and contains only very small amounts of Nb and the results show negative Nb, pointing to interference of Zr on Nb background.

The Nb Lα line lies next to Zr Lβ lines in the WDS spectrum. The negative values resulted from an overcorrection for Nb background; *i.e.*, a small portion of Zr Lβ3 peak was included in the background measurement for Nb.

We corrected the faulty values for Nb by using as a new background value for all analyses the "peak" value of the eudialyte with the lowest negative value for Nb (#70, AS12-01: −0.1431 wt % Nb_2O_5 and 2.5 cps), which likely contained very little Nb. These values are the ones given in Table 6.

The difference in Nb values minimally affected matrix corrections for the other oxides, resulting in different values at the second or third decimal: insignificant changes in the context of error intervals for the respective oxide analyses. Despite correcting the Nb values, they are still significantly lower on WDS-EMP than on SEM-EDS.

4.4. Crystal Chemistry of the Eudialyte-Group Minerals

The results of WDS-EMP analyses on eudialytes have been processed in accordance with Johnsen and Grice [23] and Pfaff *et al.* [52] along with common crystal-chemical principles, as applied by Andersen *et al.* [53,54]. Cations were thus assigned to the *N*, *M*(1), *M*(2), *M*(3), *M*(4), and *Z* sites. See Electronic Appendix 2 for the full dataset of processed eudialyte analyses.

Naming end-members is less important than understanding the crystal chemistry of the eudialyte-group minerals, however, an attempt was made to determine the dominant end-members in Norra Kärr eudialyte by following the hierarchical guidelines set up by Johnsen *et al.* [19] as far as possible and by distinguishing end-members by the cation occupancy in the *M*(1), *M*(2), and *M*(3) sites. We have only included the major end-members in this study (Tables 2 and 3).

Figure 6 presents the crystal-chemical distribution of the eudialyte-group minerals in a three-dimensional scatter plot, with projected two-dimensional scatter plots of the *M*(1), *M*(2), and *M*(3) axes. Eudialytes from similar lithologies are color coded in the 3D plot (red [ELAK], green [PGT], and purple [GTM]), but were given individual symbols in the 2D plots.

Variables for the different axes are the proportions of Ca (Ca/[Ca+REE+Mn+Fe]), Mn (Mn/[Mn+Fe]), and Nb (Nb/[Nb+Si]) in the *M*(1), *M*(2), and *M*(3) sites, respectively. One should keep in mind that of the REE only La, Ce, Nd, and Y were analyzed by WDS-EMP and that the occupancy calculated for the *M*(1) site is only a (close) approximation.

Eudialytes from Norra Kärr, based on 142 analyses from 18 different samples, can be divided into three distinct groups that correspond to the lithologic units they belong to (Table 4), as illustrated by Figures 6 and 7.

Most clearly, the three groups are distinguishable by their relative Fe and Mn content. As argued by previous authors [21,24–26], the Mn/Fe ratio is a proxy for magmatic evolution and, assuming that the relatively small Norra Kärr Alkaline Complex originated from one pulse of magma, this means that the eudialyte-group minerals may reveal clues about the sequence of crystallization of the different units.

Using Table 3, and the hierarchy of Johnsen *et al.* [19], we can tell which end-members are defined by the corners of Figure 6. For example, if a crystal has more than 50% Ca in the *M*(1) site, has Fe in the *M*(2) site, and Si in the *M*(3) site, it is the *sensu stricto* end-member eudialyte. If the *M*(3) site instead contains Nb, it is the end-member ferrokentbrooksite.

End-member discrimination in three dimensions is advantageous in this case. The corners of the projected 2D scatterplots are commonly occupied by two different end-members and there is overlap between different groups of eudialyte, making it very difficult to distinguish trends in the crystal chemistry.

Given the number of known and theoretically-possible end-members in the eudialyte group, the discrimination of different end-members and their proportions in a single crystal can be continued almost *ad infinitum* and therefore we will stick to the dominant crystal chemistry of the *M*(1), *M*(2), and *M*(3) sites and variations in the total content.

Figure 6. Three-dimensional scatterplot and projected two-dimensional scatterplots of the relative abundance of Ca (Ca/[Ca+REE+Mn+Fe]), Mn (Mn/[Mn+Fe]), and Nb (Nb/[Nb+Si]) in the *M*(1), *M*(2), and *M*(3) sites, respectively, in eudialyte-group minerals as analyzed by WDS-EMP. The corners of the three-dimensional box represent different eudialyte-group end-members. Eudialytes from Norra Kärr can be distinctly discriminated into three groups, which correspond to their respective lithologic units ELAK (red), PGT (green), and GTM (purple).

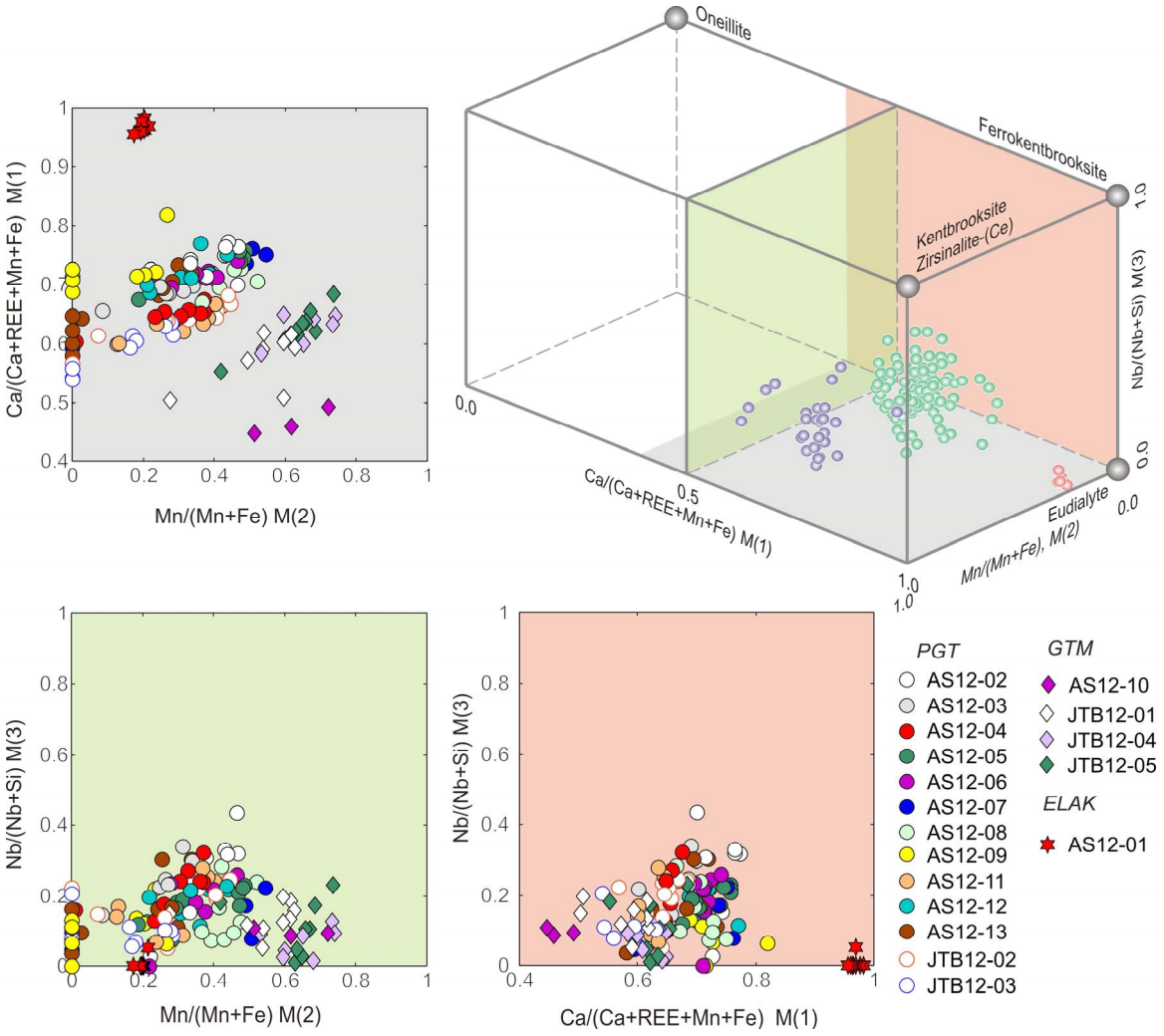

Figure 7. Ternary diagrams for eudialytes analyzed by WDS-EMP, plotting their relative total atomic content of Fe and Mn with La, Ce, Nd, and Y. The eudialytes are distinctly separated into three groups by their Fe and Mn content, which match the three lithologic units the samples were taken from: ELAK, PGT, and GTM, marked by a red, purple, and green line, respectively. La, Ce, and Nd increase with increasing Mn content; Y is most enriched in the PGT group.

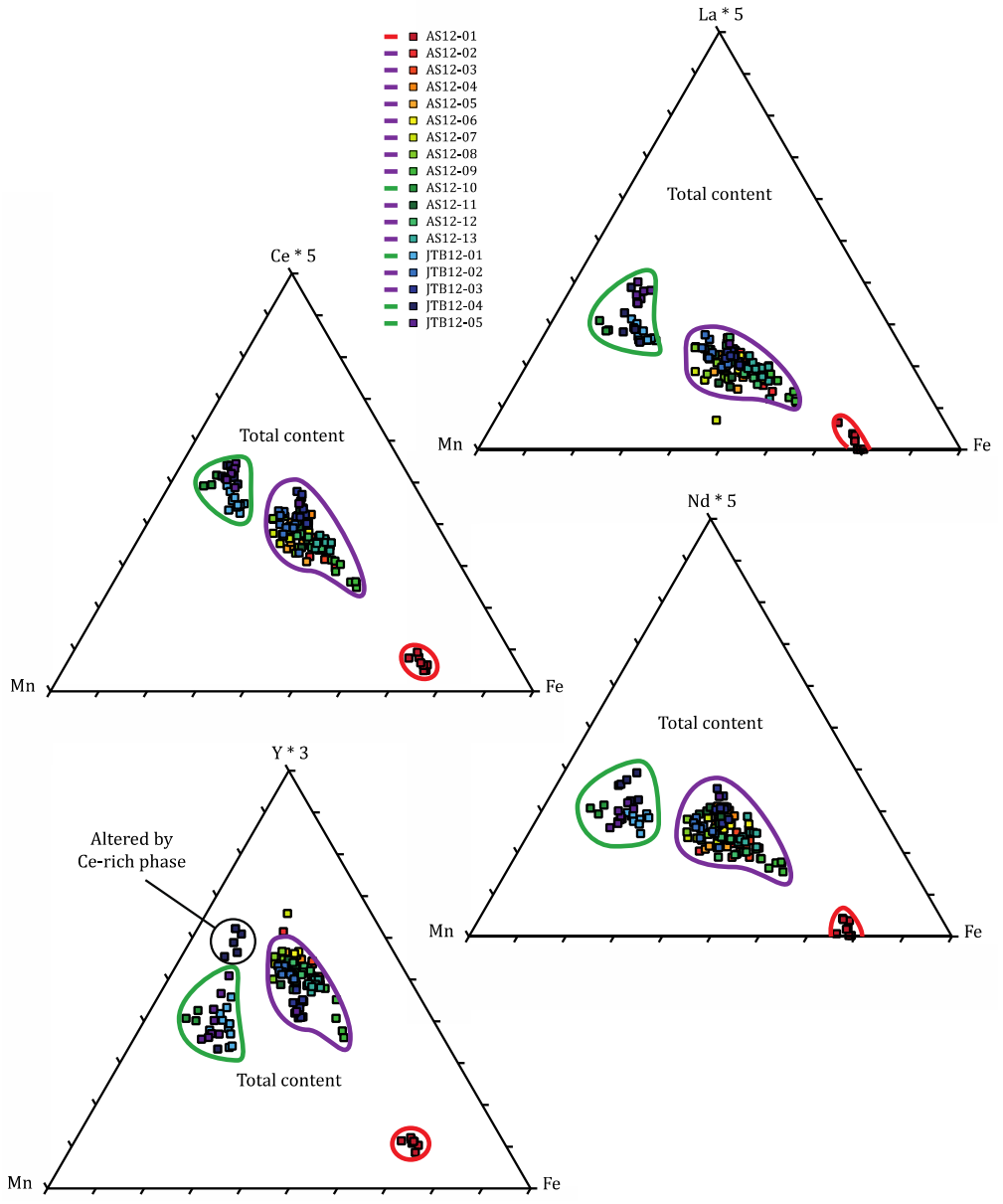

Rather than Mn/Fe (as used by other authors) we prefer using Mn/(Fe+Mn), because this gives the atomic percentage of Mn in eudialyte. In the *sensu stricto* eudialyte and kentbrooksite series Fe and Mn are held in the *M*(2) site—the primary Fe-Mn-bearing crystal site—and substitute for another to a sum of 3 *apfu*.

In order of increasing Mn/(Fe+Mn) ratio (Figures 6 and 7), we can distinguish EGM from the lakarpite unit with pink eudialyte (ELAK), "pegmatitic" grennaite (PGT), and "migmatitic" grennaite (GTM). The dominating eudialyte-group end-members of the respective lithologic units can be generalized to a *sensu stricto* eudialyte (ELAK), a Ca-poor Fe-Mn eudialyte-ferrokentbrooksite (PGT),

and a Ca-poor Mn-dominated eudialyte-kentbrooksite (GTM). Assuming that increasing Mn/(Fe+Mn) ratios in eudialyte are related to increasing degrees of magmatic differentiation, this suggests that the units crystallized in the same sequence from batches of differentiated melt belonging to a common liquid line of descent.

Figure 7 presents four triangular diagrams with WDS-EMP data for Fe and Mn in the lower corners and La, Ce, Nd, and Y in the top corners, not for any specific crystal sites. The eudialyte clusters are the same as in Figure 6, in order of increasing Mn/(Fe+Mn) ratio: ELAK, PGT, and GTM. The total content of LREE increases with an increasing Mn/(Fe+Mn) ratio and, thus, with magmatic evolution.

Y—essentially a HREE—appears to behave differently and is significantly more enriched in PGT eudialytes than in those of the GTM unit. Sample JTB12-04 (GTM) differs from the other samples from that unit, because it is being replaced by a Ce-rich phase that is seen as bright phase in eudialyte in backscattered electron images, which depletes the LREE of the eudialyte and makes it relatively richer in HREE. Thus, the relative and absolute abundance of LREE in eudialyte increases with increasing Mn/(Fe+Mn) ratio.

This observation can be transferred to whole-rock REE content (Figure 8). The GTM unit is enriched in LREE compared to the PGT unit, corresponding to the REE content of their respective eudialyte-group minerals. Eudialyte is the main REE-bearing mineral in units GTC, PGT, and GTM. In the ELAK unit most of the REE are probably accommodated in mosandrite [3], since the ELAK eudialyte contains relatively little REE.

Figure 8. Chondrite-normalised [55] whole-rock REE+Y plots of samples representative of the different lithologic units (Table 5). Note that particularly the GTM unit is relatively richer in LREE. All rocks in Norra Kärr have negative Eu anomalies, suggesting an alkali basaltic origin [1].

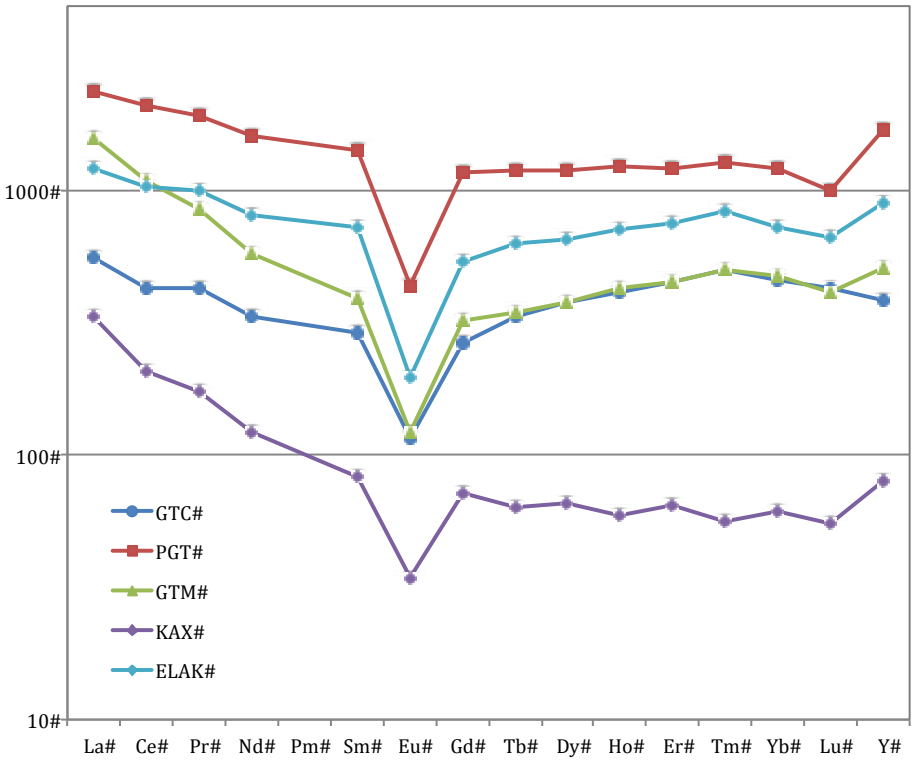

By comparison with our analyses, Fryer and Edgar [29] most likely analyzed eudialyte from the PGT unit and Schilling *et al.* [21] most likely analyzed eudialyte from the ELAK unit, based on the lower REE concentrations and the pink color of the eudialyte in hand specimen [56].

5. Conclusions

Comparison of chemical analyses of the complex mineral eudialyte by SEM-EDS and WDS-EMP reveals that, after proper set-up and calibration, SEM-EDS is generally approaching the quality of WDS-EMP. Considering the user-friendly nature of EDS and its availability on most SEM instruments, this makes SEM-EDS an important tool for reconnaissance work, preliminary analyses in research, and especially in exploration-related studies.

In the light of the new data that we present, eudialyte-group minerals from the Norra Kärr Alkaline Complex are separated into three distinct groups:

- Fe-rich, REE-poor, classical pink eudialyte from lakarpite;
- Fe-Mn-bisected, HREE-rich eudialyte from "pegmatitic" grennaite;
- Mn-rich, LREE-rich eudialyte from "migmatitic" grennaite.

The notion that any one eudialyte is representative of all eudialyte at Norra Kärr is not supported and it is more useful to see different eudialyte-group minerals in their context. Eudialyte-group minerals at Norra Kärr display a trend from low to high Mn/(Fe+Mn) ratios with a corresponding increase in absolute and relative LREE content. This trend is interpreted as a result of magmatic evolution based on the increasing Mn/(Fe+Mn) ratio. In terms of eudialyte group end-members, there is a line of evolution from a *sensu stricto* eudialyte, through a Ca-poor Fe-Mn-bisected eudialyte-ferrokentbrooksite, and finally a Ca-poor eudialyte-kentbrooksite.

Acknowledgments

First and foremost we would like to thank Tasman Metals Ltd. for their hospitality, transparence, and funding of this study; Johan Berg is thanked for his help with sampling. Julian Schilling is thanked for communication in the early stages of the experiment along with Henrik Friis, who also provided a thorough peer-review of this paper together with an anonymous referee.

References

1. Sørensen, H. The agpaitic rocks—An overview. *Mineral. Mag.* **1997**, *61*, 485–498.
2. Mindat.org, the Mineral and Locality Database Home Page. Available online: http://www.mindat.org/ (accessed on 31 May 2012).
3. Bellezza, M.; Merlino, S.; Perchiazzi, N. Mosandrite: Structureal and crystal-chemical relationships with rinkite. *Can. Miner.* **2009**, *47*, 897–908.
4. Ussing, N.V. Geology of the Country around Julianehaab, Greenland. *Meddr. Grønl.* **1912**, *38*, 1–426.
5. Sørensen, H. On the Agpaitic Rocks. In *Report of the International Geological Congress 21st Session Norden*, Copenhagen, Denmark, 15–25 August 1960; Volume 13, 319–327.
6. Le Maitre, R.W. *Igneous Rocks: A Classification and Glossary of Terms*, 2nd ed.; Cambridge University Press: Cambridge, UK, 2002.

7. Sørensen, H., Ed. *The Alkaline Rocks*, 1st ed.; John Wiley: London, UK, 1974.
8. Marks, M.A.W.; Hettmann, K.; Schilling, J.; Frost, B.R.; Markl, G. The mineralogical diversity of alkaline igneous rocks: Critical factors for the transition from miaskitic to agpaitic phase assemblages. *J. Petrol.* **2011**, *52*, 439–455.
9. Ferguson, J. Geology of the Ilímaussaq alkaline intrusion, South Greenland: Description of map and structure. *Bull. Grønl. Geol. Undersøgelse* **1964**, *39*, 1–82.
10. Sørensen, H. The Ilímaussaq alkaline complex, South Greenland—An overview of 200 years of research and an outlook. *Meddr. Grønl.* **2006**, *45*, 1–70.
11. Gerasimovsky, V.I.; Volkov, V.P.; Kogarko, L.N.; Polyakov, A.I. Kola Peninsula. In *The Alkaline Rocks*, 1st ed.; Sørensen, H., Ed.; John Wiley: London, UK, 1974; pp. 206–221.
12. Philpotts, A.R. The Monterregian Province. In *The Alkaline Rocks*; Sørensen, H., Ed.; John Wiley: London, UK, 1974; pp. 293–310.
13. Schilling, J.; Marks, M.A.W.; Wenzel, T.; Vennemann, T.; Horváth, L.; Tarassoff, P.; Jacob, D.E.; Markl, G. The magmatic to hydrothermal evolution of the intrusive mont saint-hilaire complex: Insights into the late-stage evolution of peralkaline rocks. *J. Petrol.* **2011**, *52*, 2147–2185.
14. Salvi, S.; Fontan, F.; Monchoux, P. Hydrothermal mobilization of high field strength elements in alkaline igneous systems: Evidence from the Tamazeght Complex (Morocco). *Econ. Geol.* **2000**, *95*, 559–576.
15. Verwoerd, W.J. The Pilanesberg Alkaline Province. In *The Geology of South Africa*; Johnson, M.R., Anhaeusser, C.R., Thomas, R.J., Eds.; Geological Society of S.A., Johannesburg and Council for Geoscience: Pretoria, South Africa, 2006; pp. 381–393.
16. Brøgger, W.C. Die Mineralien der Syenitpegmatitgänge der südnorwegischen Augit- und Nephelinsyenite [in German]. *Z. Krystallographie* **1890**, 1–235,1–663.
17. Larsen, A.O. *The Langesundsfjord. History, Geology, Pegmatites, Minerals*; Bode: Salzhemmerdorf, Germany, 2010.
18. Stromeyer, F. Summary of meeting 16 December 1819 (Analyse einiger grönlandischen, von Prof Giesecke erhaltenen Fossilien). *Göttingische Gelehrt. Anz.* **1819**, *3*, 1993–2000.
19. Johnsen, O.; Ferrarris, G.; Gault, R.A.; Grice, J.D.; Kampf, A.R.; Pekov, I.V. The nomenclature of eudialyte-group minerals. *Can. Miner.* **2003**, *41*, 785–794.
20. Mindat.org the Mineral and Locality Database Web Page. Eudialyte Group. Available online: http://www.mindat.org/min-11021.html (accessed on 31 May 2012).
21. Schilling, J.; Wu, F.-Y.; McCammon, C.; Wenzel, T.; Marks, M.A.W.; Pfaff, K.; Jacob, D.E.; Markl, G. The compositional variability of eudialyte-group minerals. *Miner. Mag.* **2011**, *75*, 87–115.
22. Rastsvetaeva, R.K. Structural mineralogy of the eudialyte group: A review. *Crystallogr. Rep.* **2007**, *52*, 47–64.
23. Johnsen, O.; Grice, J.D. The crystal chemistry of the eudialyte group. *Can. Miner.* **1999**, *37*, 865–891.
24. Johnsen, O.; Gault, R.A. Chemical variation in eudialyte. *Neues Jahrb. Miner.* **1997**, *171*, 215–237.

25. Pfaff, K.; Krumrei, T.; Marks, M.; Wenzel, T.; Rudolf, T.; Markl, G. Chemical and physical evolution of the lower layered sequence from the syenitic Ilímaussaq intrusion, South Greenland: Implications for the origin of magmatic layering in peralkaline felsic liquids. *Lithos* **2008**, *106*, 280–296.
26. Schilling, J.; Marks, M.; Wenzel, T.; Markl, G. Reconstruction of magmatic to subsolidus processes in an agpaitic system using eudialyte textures and composition: A case study from Tamazeght, Morocco. *Can. Miner.* **2009**, *47*, 351–365.
27. Törnebohm, A.E. Katapleiit-syenit, en nyupptäckt varietet af nefelinsyenit i Sverige [in Swedish]. *SGU Ser. C* **1906**, *199*, 1–54.
28. Google Images. Available online: http://images.google.com/ (accessed 16 August 2012).
29. Fryer, B.J.; Edgar, A.D. Significance of rare earth distributions in coexisting minerals of peralkaline undersaturated rocks. *Contrib. Miner. Petrol.* **1977**, *61*, 35–48.
30. Christensson, U. Characterising the Alteration of the Contact to the Norra Kärr Alkaline Complex, Southern Sweden. Bachelor's Thesis, University of Gothenburg, Gothenburg, Sweden, 2013.
31. Blaxland, A.B. Agpaitic magmatism at Norra Kärr? Rb-Sr isotopic evidence. *Lithos* **1977**, *10*, 1–8.
32. Welin, E. Tabulation of recalculated radiometric ages published 1960–1979 for rocks and minerals in Sweden. *GFF* **1980**, *101*, 309–320.
33. Ranjer, S. Describing and Characterising the Mylonites in the Area of the Norra Kärr Alkaline Complex, Southern Sweden. Bachelor's Thesis, University of Gothenburg, Gothenburg, Sweden, 2013.
34. Högdahl, K., Andersson, U.B., Eklund, O.. *The Transscandinavian Igneous Belt (TIB) in Sweden: A Review of Its Character and Evolution*; Geological Survey of Finland Special Paper 37; Geological Survey of Finland: Espoo, Finland, 2004.
35. Adamson, O.J. The petrology of the Norra Kärr district: An occurrence of alkaline rocks in southern Sweden. *GFF* **1944**, *437*, 113–255.
36. Von Eckermann, H. The Alkaline rocks of Norra Kärr. In *Alkaline Rocks and Minerals Deposits of Southern, Central, and Northern Sweden: Guide to Excursion No C 27*, Proceedings of International Geological Congress XXI Session Norden, Copenhagen, Denmark, 15–25 August 1960; Geological Survey of Sweden: Uppsala, Sweden, 1960; pp. 3–6.
37. Von Eckermann, H. New contributions to the interpretation of the genesis of the norra kärr alkaline body in southern Sweden. *Lithos* **1968**, *1*, 76–88.
38. Koark, H.J. Zum gefügeverhalten des nephelins in zwei vorkommen alkaliner kristaliner schiefer [in German]. *Bull. Geol. Inst. Upps.* **1960**, *39*, 1–31.
39. Koark, H.J. Zu hülle, inhalt, gefüge und alter des alkaligesteinsvorkommen von Norra Kärr im südlichen mittelschweden [in German]. *GFF* **1968**, *91*, 159–184.
40. Kramm, U.; Koark, H.J. Isotopic composition of galena lead from the Norra Kärr peralkaline complex, Sweden. *GFF* **1988**, *110*, 311–316.
41. Sood, M.K.; Edgar, A.D. Melting relations of undersaturated Alkaline rocks from the Ilímaussaq Intrusion and Grønnedal-Íka complex, South Greenland: Under water vapour and controlled partial oxygen pressure. *Meddr. Grønl.* **1970**, *181*, 1–41.

42. Piotrowski, J.M.; Edgar, A.D. Melting relations of undersaturated Alkaline rocks from South Greenland compared to those of Africa and Canada. *Meddr. Grønl.* **1970**, *181*, 1–62.
43. Whitney, D.L.; Evans, B.W. Abbreviations for names of rock-forming minerals. *Am. Miner.* **2010**, *95*, 185–187.
44. Thulin, H. Norra Kärr: Avsnitt 1 [in Swedish]. *Litofilen* **1996**, *1*, 17–27.
45. Tasman Metals Ltd. Web Page. Norra Kärr Rare Element Project. Available online: http://www.tasmanmetals.com/s/Norra-Karr.asp (accessed on 25 June 2012).
46. ALS Limited. Minerals: Method description ME-MS81. Available online: http://www.alsglobal.com/upload/minerals/downloads/method-descriptions/Method%20Descriptions-ME-MS81.pdf (accessed on 16 July 2012).
47. ALS Limited. Minerals: Method description ME-ICP06. Available online: http://www.alsglobal.com/upload/minerals/downloads/method-descriptions/Method-Descriptions-ME-ICP06.pdf (accessed on 2 October 2012).
48. Jarosewich, E.; Boatner, L.A. Rare-earth element reference samples for electron microprobe analysis. *Geost. Newsl.* **1991**, *15*, 397–399.
49. Pouchou, J.L.; Pichoir, F. A new model for quantitative X-ray microanalysis. I. Application to the analysis of homogeneous samples. *Rech. Aerosp.* **1984**, *3*, 13–38.
50. Microanalysis Consultants Home Page. Available online: http://www.macstandards.co.uk (accessed on 14 March 2013).
51. SPI Supplies Web Page. SPI off—The Shelf Microanalysis Standards. Available online: http://www.2spi.com/catalog/standards/spiweb/micro.html (accessed on 14 March 2013).
52. Pfaff, K.; Wenzel, T.; Schilling, J.; Marks, M.A.W.; Markl, G. A fast and easy-to-use approach to cation site assignment for eudialyte-group minerals. *N. Jahrbuch Miner. Abh.* **2010**, *187*, 69–81.
53. Andersen, T.; Erambert, M.; Larsen, O.A.; Selbekk, R.S. Petrology of nepheline syenite pegmatites in the Oslo Rift, Norway: Zirconium silicate mineral assemblages as indicators of alkalinity and volatile fugacity in mildly agpaitic magma. *J. Petrol.* **2010**, *51*, 2303–2325.
54. Andersen, T.; Erambert, M.; Larsen, O.A.; Selbekk, R.S. Petrology of nepheline syenite pegmatites in the Oslo Rift, Norway: Zr and Ti mineral assemblages in miaskitic and agpaitic pegmatites in the Larvik Plutonic Complex. *Mineral. Pol.* **2012**, doi:10.2478/v10002-012-0001-7.
55. Taylor, S.R.; McLennan, S.M. *The Continental Crust: Its Composition and Evolution*; Blackwell: Oxford, UK, 1985.
56. Schilling, J. Geological Survey of Norway, Trondheim, Norway. Personal communication, 2 March 2012.